ISBN: 978-3-95450-222-6 ISSN: 2673-5350 doi:10.18429/JACoW-IBIC2020-WEPP05

REENTRANT CAVITY RESONATOR AS A BEAM CURRENT MONITOR (BCM) FOR A MEDICAL CYCLOTRON FACILITY*

S. Srinivasan†, P.-A. Duperrex, J. M. Schippers
Paul Scherrer Institut, 5232 Villigen PSI, Switzerland

Abstract

At PSI, a dedicated proton therapy facility, with a superconducting cyclotron, delivers 250 MeV beam energy, pulsed at 72.85 MHz. The measurement of beam currents (0.1-10 nA) is generally performed by ionisation chambers (ICs), but at the expense of reduced beam quality, and scattering issues. There is a strong demand to have accurate signal with a minimal beam disturbance. A cavity resonator, on fundamental resonance mode, has been built for this purpose. The cavity, coupled to the second harmonic of the pulse rate, provides signals proportional to the beam current. It is installed in a beamline to measure for the energy range 238-70 MeV. Good agreement is reached between the expected and measured sensitivity of the cavity. The cavity delivers information for currents down to 0.15 nA with a resolution of 0.05 nA when integrated over one second. Its application is limited to a machine-safety monitor to trigger interlocks, within the existing domain of the proton therapy due to the low beam current limits. With new advancements in proton therapy, especially FLASH, the cavity resonator's application as an online beam-monitoring device is feasible.

INTRODUCTION

In proton radiation therapy at PSI, proton beams of low intensities (0.1-10 nA) are traditionally measured with ICs [1]. We face a strict regulation of their use due to scattering issues. A non-invasive BCM, is modelled as a lumped element LC circuit, such that its fundamental mode of resonance is at 145.7 MHz as described in [2]. The induced electric and magnetic fields are concentrated in the capacitive (region 2) and the inductive zones (region 3) of the BCM, as shown in Figure 1. Here, we report on its beamline measurements for the energy range 238-70 MeV.

BCM LOCATION

The proton therapy facility, PROSCAN, is a temperature-controlled environment (28.5±0.5 °C), to have stable operating conditions for its beamline elements. The energy degradation (238-70 MeV), is achieved with the help of a degrader [3], which results in growth of emittance and energy spread [4-6]. An Energy Selection System (ESS), along with a pair of collimators, maintains the beam quality at patient location by limiting the energy spread. An elongation of the proton bunch length and an energy dependent decrease in the bunch amplitude downstream of the degrader is the consequence. This affects the BCM's sensitivity as it is coupled to the second harmonic of the pulse repetition rate, which is located at sixteen meters from the degrader exit as shown in Figure 2.

A Sinc function normalised to average beam current and at multiple energies is given in Table 1, represents the BCM's expected second harmonic amplitude factor, A_2, proportional to the sensitivity.

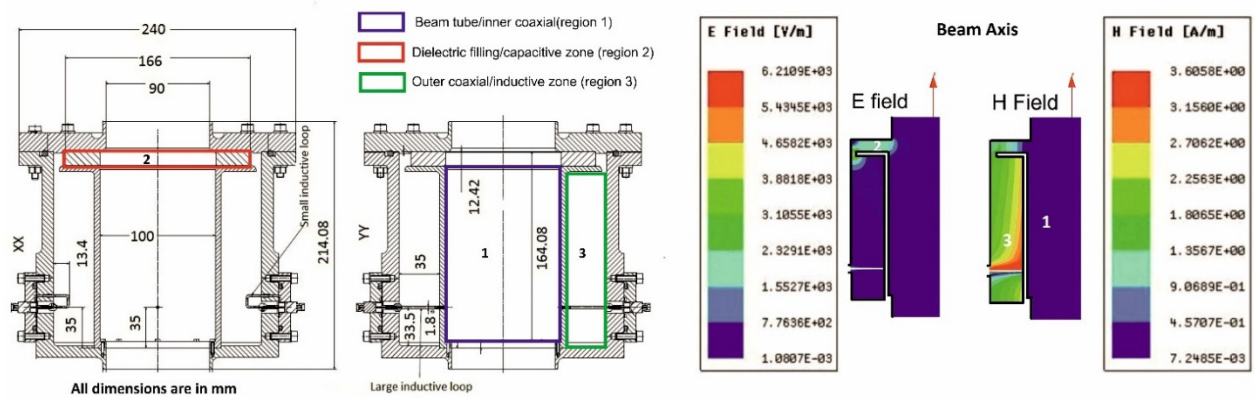

Figure 1: Cut-section of the reentrant cavity resonator (XX and YY) with dimensions correpsonding to TM_{010} frequency at 145.7 MHz. Region 1, 2 and 3 represent the inner coaxial (or beam tube), dielectric filling in the reentrant gap (capacitive zone), and the outer coaxial (inductive zone). The E fields and H fields excited within the resonator shows the separation of the capacitive (marked as 2) and inductive zones (marked as3) in this resonator (right).

* This project has received funding from the European Union's Horizon 2020 research and innovation programme under the Marie Skłodowska-Curie grant agreement No 675265.
† sudharsan.srinivasan@psi.ch

ISBN: 978-3-95450-222-6 ISSN: 2673-5350 doi:10.18429/JACoW-IBIC2020-WEPP05

Table 1: Estimate of the Second Harmonic Amplitude Factor for a Rectangular Bunch Shape [7] at the Resonator Location for Different Beam Energies. Bunch length of 2 ns at the degrader exit is assumed as reference for the calculation. Only for energies lower than 180 MeV, the ESS helps in minimising the momentum spread to ± 1%. Energy spread is calculated as per [8] and is within acceptable range of the measurement as given in [9].

Energy, MeV	Energy Spread, MeV	Momentum Spread, %	Bunch Length at Resonator, ns	2nd Harmonic Amplitude Factor (A_2)
79	4.4	1.0	3.24	0.67
109	4.2	1.0	3.08	0.69
139	3.9	1.0	2.97	0.71
171	3.3	1.0	2.91	0.73
201	2.7	0.84	2.71	0.76
231	1.7	0.70	2.56	0.79

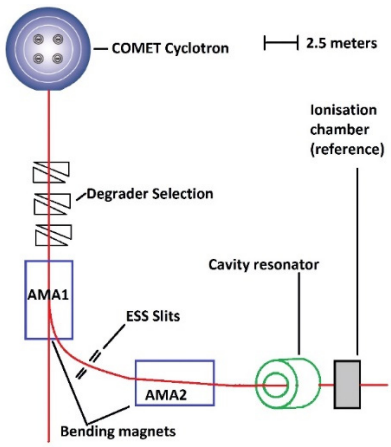

Figure 2: Location of the cavity resonator in the PROSCAN layout. Marked are the COMET cyclotron, degrader selection, ESS for momentum spread, bending magnets, cavity resonator and the IC which is used as beam current reference.

MEASUREMENT CHAIN

A PSI developed measurement system, VME MESTRA, as shown in Figure 3, is used for beam current measurements [10]. The measurement system is configured at 145.7 MHz and starts with a large inductive loop of the BCM. The other large inductive loop is connected to a resonance trombone for tuning capabilities. The pair of the small inductive loops are terminated with 50 Ω.

The cavity signal is amplified with a low-noise amplifier [11] and bandpass filtered with a customized cavity type filter from KL microwave. The centre frequency of the bandpass filter is 145.0 MHz with a 3dB bandwidth of 8.24 MHz. The filtered signal is amplified further with a FEMTO wideband low-noise amplifier [12]. This signal is digitized with the help of a 16-bit Digitizer [13] at 50.0 MSamples/s. The digitized signal is down-converted through a Field Programmable Gate Array (FPGA) on the Digital Down Converter (DDC). The DDC results in an output signal, Res DDC, with 50 k samples/s. The DDC filters the input noise power of the digitized signal with its 18 kHz (3 dB) bandwidth in order to get a high attenuation for the stop band and a flat pass band. The signal integration time of the measurement chain is one second.

RESULTS

No Beam System-response

Prior to beam measurements, the no beam response of the system is measured without the BCM and with the BCM (scenario 1 and 2 in Figure 3) with the cyclotron RF turned on. The measurement without the BCM and with the BCM were recorded as 40000 counts and 63007 counts respectively, with a standard deviation of 1.26%. This value is the measurement offset, $I_{measoff}$, that represents the noise floor of the measurement chain and its RF interference.

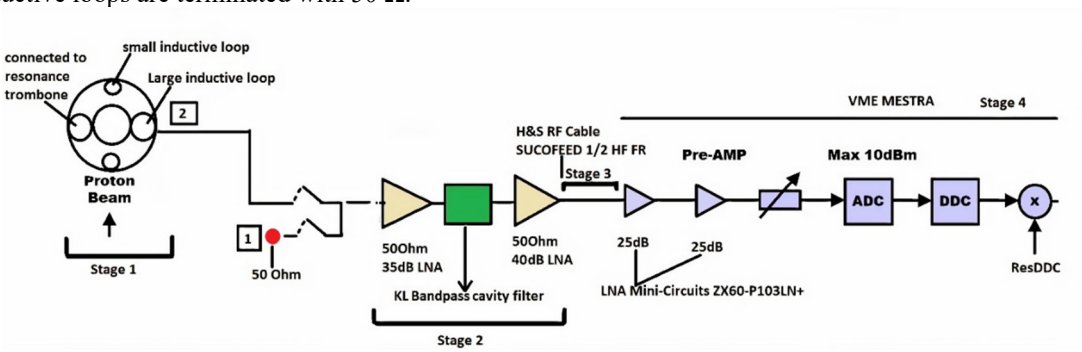

Figure 3: Measurement chain representation from the resonator until the electronic cubicle. The small inductive loops are terminated with 50 Ω. Scenario 1 represents 50Ω on the input of the measurement chain represents Stage 2-4. Scenario 2 represents the resonator connected to the measurement chain represents Stage 1-4.

ISBN: 978-3-95450-222-6 ISSN: 2673-5350 doi:10.18429/JACoW-IBIC2020-WEPP05

Table 2: Measurement Summary for Resonator at Different Energies. The fractional uncertainty of the evaluated measurement offset and the resonator calibration factor are derived from the in-beam measurements through error propagation. The value of the normalizing term, C=212042 Counts/Na. A_2, is taken from Table 1.

Proton Beam Energy (MeV)	Measured Resonator Sensitivity, k_meas (±1.35%) (Counts/nA)	Expected Resonator Sensitivity, k (=A_2*C) (Counts/nA)	Measurement Offset, $I_{measoff}$ (±1.26%) (Counts)
79	138202	142068	62418
109	139821	146309	63008
139	151327	150550	62737
171	153493	154791	62169
201	161152	161152	62104
231	168434	167513	60308

Beam Measurements

The BCM response is measured for beam current sweeps in the range 0-2.5 nA at different energies. The calibration of the BCM is performed with respect to an IC as shown in Figure 2, immediately behind the BCM to have similar beam current values. For the low beam current range a linear relationship exists between the beam current power and the measured signal power, which is given by

$$I^2_{\mathrm{Re}sDDC} = I^2_{measoff} + k^2 I^2_{beam} \quad (1)$$

where the individual power of the measurement offset ($I^2_{measoff}$) and the power of the beam current response ($k^2I^2_{beam}$) are uncorrelated, with k as the BCM sensitivity. The measurement results are summarised in Table 2 and are in good agreement with the expected sensitivity and the measurement offset from the no beam response. The measurement from the BCM is considered position independent as its position dependence is 0.03%/mm measured at 60% of the beam pipe radius.

The lowest detectable beam current, is 0.15 nA, which is defined by a signal level higher than the measurement offset by three σ. The resolution derived from the measurement is 0.05 nA.

The cavity BCM will be used as a beam operation safety monitor as well as in controlling the operation parameters within the normal ranges. With recent trend towards FLASH therapy, the cavity BCM can be used for online beam monitoring as the beam current is in the range of hundreds of nA [14].

CONCLUSION

In this work, to our knowledge, we have demonstrated the first successful non-invasive beam current measurements at a proton therapy facility in the range 0.1-10 nA.

ACKNOWLEDGMENT

The authors like to thank the vacuum group and the PROSCAN maintenance group for installation in the beamline.

REFERENCES

[1] R. Dölling, "Progress of the diagnostics at the PROSCAN beam lines," in *Proc. 8th European Workshop on Beam Diagnostics and Instrumentation for Particle Accelerators (DIPAC'07)*, Venice, Italy, May 2007, pp. 361–363.

[2] S. Srinivasan and P.-A. Duperrex, "Dielectric-filled reentrant cavity resonator as a low-intensity proton beam diagnostic," *Instruments*, vol. 2, no. 4, article no. 24 (17 pages), 2018. doi:10.3390/instruments2040024

[3] V. Rizzoglio *et al.*, "Evolution of a beam dynamics model for the transport line in a proton therapy facility," *Phys. Rev. Accel. Beams*, vol. 20, no. 12, pp. 1–12, 2017. doi:10.1103/PhysRevAccelBeams.20.124702

[4] F. J. M. Farley, "Optimum strategy for energy degraders and ionization cooling," *Nucl. Instrum. Meth.. A*, vol. 540, pp. 235–244, 2005. doi:10.1016/j.nima.2004.11.034

[5] V. Anferov, "Energy degrader optimization for medical beam lines," *Nucl. Instrum, Meth. A*, vol. 496, no. 1, pp. 222–227, 2003. doi:10.1016/S0168-9002(02)01625-X

[6] J. Petzoldt *et al.*, "Characterization of the microbunch time structure of proton pencil beams at a clinical treatment facility," *Phys. Med. Biol.*, vol. 61, no. 6, pp. 2432–2456, 2016. doi:10.1088/0031-9155/61/6/2432

[7] R. E. Shafer, "Beam position monitoring," *AIP Conf. Proc.*, vol. 212, pp. 26–58, 1990. doi:10.1063/1.39710

[8] P. Vavilov, "Ionization losses of high-energy heavy particles," *Sov. Phys. JETP*, vol. 5, no. 4, pp. 749–751, 1957.

[9] M. J. Van Goethem, R. Van Der Meer, H. W. Reist, and J. M. Schippers, "Geant4 simulations of proton beam transport through a carbon or beryllium degrader and following a beam line," *Phys. Med. Biol.*, vol. 54, no. 19, pp. 5831–5846, 2009. doi:10.1088/0031-9155/54/19/011

[10] E. Johansen, "VME MESTRA Rev C Specification," 2020. doi:10.5281/zenodo.3887550 [11]"R&K-LA100-0S Low Noise Amplifier," http://www.rk-microwave.com/jp/products/pdf/LA101-0S_01.pdf (accessed Jan. 16, 2020).

[12] FEMTO, "Datasheet Ultra-Wideband Voltage Amplifier DUPVA-1-70 Variable-Gain," http://www.femto.de (accessed Jan. 15, 2020).

[13] "ADC _ 3110 / 3111 – Eight Channel 16-bit ADC Data Sheet," https://www.ioxos.ch/produit/adc-3110-3111/ (accessed Jan. 15, 2020).

[14] A. Patriarca *et al.*, "Experimental Set-up for FLASH Proton Irradiation of Small Animals Using a Clinical System," *Int. J. Radiat. Oncol. Biol. Phys.*, vol. 102, no. 3, pp. 619-626, 2018. doi:10.1016/j.ijrobp.2018.06.403